

Vibrations of a water adlayer on Ru(0001)

Peter J. Feibelman

Sandia National Laboratories, Albuquerque, New Mexico 87185-1413

(Received 8 August 2002; published 28 January 2003)

Ab initio vibration spectra have been calculated for two-dimensional arrangements of intact and partially dissociated water molecules adsorbed on Ru(0001) and for an ice-Ih crystal. Dissociation of the non-hydrogen-bonding O-D bonds of a heavy-water bilayer on Ru(0001) eliminates the highest-energy O-D stretch feature, just as is seen in Denzler *et al.*'s (unpublished) sum frequency generation observations. Reduced zero-point energy, a consequence of replacing O-D stretch vibrations with softer Ru-D modes, stabilizes partially dissociated adlayers relative to adsorption structures made purely of intact water molecules.

DOI: 10.1103/PhysRevB.67.035420

PACS number(s): 68.43.Pq

I. INTRODUCTION

Water-surface interactions govern aqueous heterogeneous chemistry, flow through nanoscale channels, adhesion, and brittle fractures in humid environments, a host of biological and geophysical phenomena, formation of raindrops in the upper atmosphere, etc., a virtually endless list. Broad-ranging success in interpreting condensed-matter atomic geometries raises the hope that *ab initio* electronic-structure calculations based on density-functional theory¹ (DFT) in the generalized gradient approximation² (GGA) will faithfully describe the nature of the water-solid interface. But there is reason to be skeptical. Water is a closed-shell molecule, and therefore interacts relatively weakly with its environment. DFT is most reliable for strongly interacting systems.

Crystals on which water adsorbs periodically should allow the least ambiguous tests of the DFT/GGA description of water-surface interactions. Of these,³ atomic positions have only been extracted from diffraction data for D₂O/Ru(0001),⁴ which is accordingly the logical case to study first.

Depositing heavy water on Ru(0001), then annealing carefully, Held and Menzel found they could produce a $\sqrt{3} \times \sqrt{3}$ -R30° superlattice with two D₂O's and three surface Ru atoms per surface unit cell.⁴ By analyzing low-energy electron-diffraction (LEED) intensity vs beam energy from this periodic overlayer, they determined the positions of both the O and the surface-layer Ru atoms, relative to the underlying metal.

Because D atoms scatter low-energy electrons weakly, Held and Menzel drew no conclusions regarding deuterium positions, implicitly leaving the way in which D₂O bonds to Ru open to speculation. Such speculation was warranted by the surprising results of their analysis. Held and Menzel had anticipated that the first D₂O's on the Ru surface would arrange in an icelike "bilayer" (see Fig. 1), with O atoms lying in two planes separated by ~ 1 Å. Instead, their analysis implied that the O atoms of the $\sqrt{3} \times \sqrt{3}$ -R30° D₂O/Ru(0001) adlayer are virtually coplanar, lying in planes separated by only ~ 0.1 Å.

Reasoning on the basis of extensive GGA calculations, I recently proposed that this unexpected result corresponds to an adsorption structure in which half the admolecules are

dissociated, forming an H-bonded layer of OD and D₂O on the Ru(0001) surface, and the remaining D atoms are bonded directly to the metal.⁵ (see Fig. 2) This proposal was supported by both geometric and energetic results. GGA optimization of icelike bilayers produced structures in which O atoms lie in two planes separated by 0.5–1.0 Å. In contrast, the lowest-energy configuration of a half-dissociated adlayer has virtually coplanar O atoms (see Fig. 2). In addition, the binding energies of icelike two-dimensional water adlayers were consistently ~ 0.2 eV smaller than the sublimation energy of ice-Ih, implying that an icelike first water layer is not only incompatible with the LEED structure analysis,⁴ but also thermodynamically unstable against rearranging into a three-dimensional ice crystal. In contrast, the adsorption enthalpy of the half-dissociated adlayer was virtually equal to the sublimation energy of ice-Ih, excluding zero-point energy in both cases. This suggested that it, or a closely related structure, is what wets Ru(0001).

Denzler *et al.*⁶ have lent weight to the notion of a half-dissociated wetting layer, reporting recently that as they thermally desorbed all but the last of several D₂O layers from a Ru(0001) surface, an initially strong, "free O-D" (cf. Fig. 1) vibration feature at 2730 cm⁻¹ disappeared entirely from their sum frequency generation (SFG) signal. Their interpretation, that there are no non-H-bonding O-D bonds left in the first water layer on Ru(0001), is evidently consistent with the half-dissociated structure shown in Fig. 2.

With vibration spectroscopy appearing to confirm the GGA prediction of wetting-layer structure, direct comparison of GGA total-energy calculations and vibration measurements is timely. I have therefore computed approximate vibrational densities of states for a half-dissociated wetting layer, for an intact-water-molecule bilayer, and for bulk ice-Ih. I report these vibration spectra in Sec. IV B of this paper and discuss them in comparison both with Ref. 6 and with Thiel, DePaola, and Hoffman's⁷ early electron energy-loss spectroscopy (EELS) study of H₂O/Ru(0001).

The reliability of the GGA spectra is supported by $\sim 1\%$ agreement between calculated and observed "free" OD vibration frequencies, and also by a comparison of theoretical and measured vibration bands for bulk ice-Ih. Thus, evidence is accumulating that the GGA provides a reliable description of the water-Ru interaction. The calculated spectra are ac-

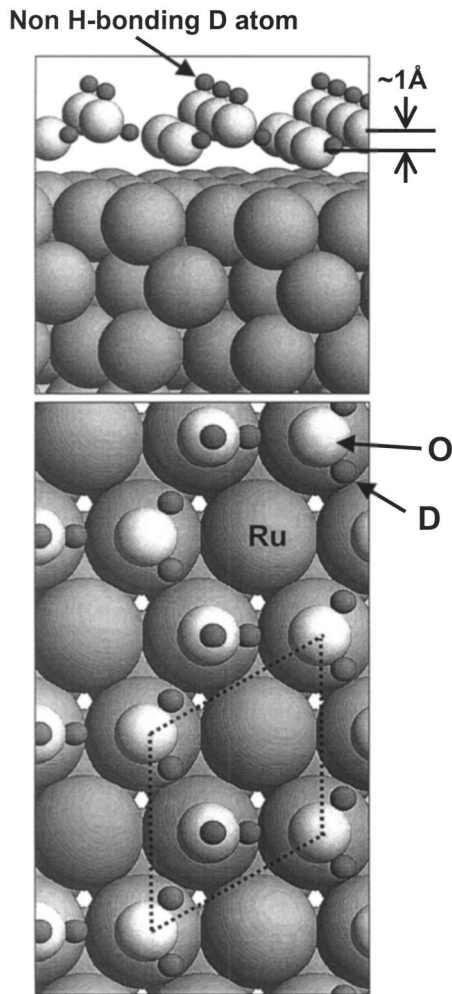


FIG. 1. The heavy-water bilayer geometry expected for $\text{D}_2\text{O}/\text{Ru}(0001)$. Upper panel: A side view. The $\sim 1\text{-}\text{\AA}$ separation between the O atom planes of the bilayer is indicated. The upper D_2O 's contribute one of their D atoms to the H-bonding network. The other is non-H bonding, as indicated. Lower panel: Top view of the bilayer. The dotted parallelogram denotes the $\sqrt{3}\times\sqrt{3}\text{-}R30^\circ$ surface unit cell. Arrows identify the atom species.

cordingly a resource for further experimental confirmation of a half-dissociated wetting layer.

Beyond that, the theoretical spectra can be used to learn how zero-point energy affects the heats of adsorption of potential wetting-layer structures and their stability relative to ice-Ih. This is the subject of Sec. V below. I show there that the replacement of stiff O-D bonds with softer Ru-D bonds lowers the energy of the half-dissociated layer by over 50 meV/ D_2O molecule relative to a bulk ice crystal. This result implies that at a typical experimental temperature $T = 150\text{ K}$ or $k_B T \sim 13\text{ meV}$, close to 100% of a $\text{Ru}(0001)$ surface is covered by a two-dimensional half-dissociated overlayer rather than three-dimensional ice mounds. In contrast, the zero-point contribution to the heat of adsorption of an intact-molecule bilayer is too small to allow it to wet the metal.

The remainder of this paper is organized as follows: In Sec. II, I discuss the numerical methods used to obtain dy-

namical matrices and compute vibration spectra. Section III concerns the best choice of unit cell to represent a water adsorption structure in which OD (or OH) -bond orientations are likely to be disordered. Section IV A is devoted to tests of the numerical and physical approximations used, and Sec. IV B to presentation and discussion of the computed spectra. In Sec. V A I discuss various theoretical issues concerning the evaluation of wetting-layer zero-point energies, and in Sec. V B, I present and discuss the zero-point energy results. Section VI is a brief recapitulation.

II. NUMERICAL METHODS

To obtain dynamical matrices for Hooke's law calculations of vibration frequencies, I used VASP,⁸⁻¹¹ an efficient plane-wave implementation of DFT, and the Perdew-Wang 1991 GGA,² which gives a reasonable account of the binding and elastic properties of bulk ice-Ih. Plane-wave calculations involving Ru, H, or D and especially O atoms can require large basis sets. This requirement is mitigated in VASP by the use of ultrasoft pseudopotentials¹²⁻¹⁵ (USP's) or, for greater accuracy, the projector augmented wave (PAW), all-electron description of the electron-ion-core interaction.^{16,17} The results reported here are mostly based on using USP's with a 29.1-Ry cutoff. I used PAW potentials together with a 51-Ry cutoff to spot check convergence, as noted below.

In all the adlayer calculations, I modeled semi-infinite $\text{Ru}(0001)$ as a slab five layers thick. To find ground-state geometries, I fixed the Ru atoms of the lower three layers at *ab initio*, bulk Ru relative positions ($a = 2.72$, $c = 4.30\text{ \AA}$), then relaxed the remaining atoms till forces on them were $< 0.03\text{ eV/\AA}$.

I confined the computation of dynamical matrices to the Γ points in the phonon surface Brillouin zones (SBZ's) of a $\sqrt{3}\times\sqrt{3}\text{-}R30^\circ$ surface unit cell containing two water molecules and, aiming to estimate dispersive effects, a $3\times 3\sqrt{3}$ cell (equivalent to two 3×3 cells) containing twelve. In the end, the $3\times 3\sqrt{3}$ calculations proved important beyond the question of dispersion, because the optimal GGA O-O distances in this cell differ from those of the $\sqrt{3}\times\sqrt{3}\text{-}R30^\circ$ cell by a few hundredths of an angstrom (cf. Fig. 3). Since the potential in which an H-bonding D atom vibrates depends on the separation of its closest two O-atom neighbors, this shifts vibration frequencies by tens of cm^{-1} .

I used a 4×4 set of equally spaced k vectors to sample the electronic surface Brillouin zone of the $\sqrt{3}\times\sqrt{3}\text{-}R30^\circ$ cell and a 2×2 set for the $3\times 3\sqrt{3}$ calculations. I accelerated electronic relaxation with Methfessel and Paxton's Fermi-level smearing method (width = 0.2 eV),¹⁸ and corrected for the contact potential difference associated with having an adlayer on only one side of an Ru slab using Kresse's adaptation¹⁹ of Neugebauer and Scheffler's method.²⁰

To compute Hooke's law dynamical matrices at the point Γ , I displaced O or D nuclei from their equilibrium sites by 0.00, ± 0.025 , and $\pm 0.050\text{ \AA}$ in each Cartesian direction, and extracted the force derivative by fitting the resulting restoring forces to a polynomial. To make the calculations tractable, I assumed that the Ru atoms, which are about 6.3 times more massive than O, do not move as the O atoms vibrate.

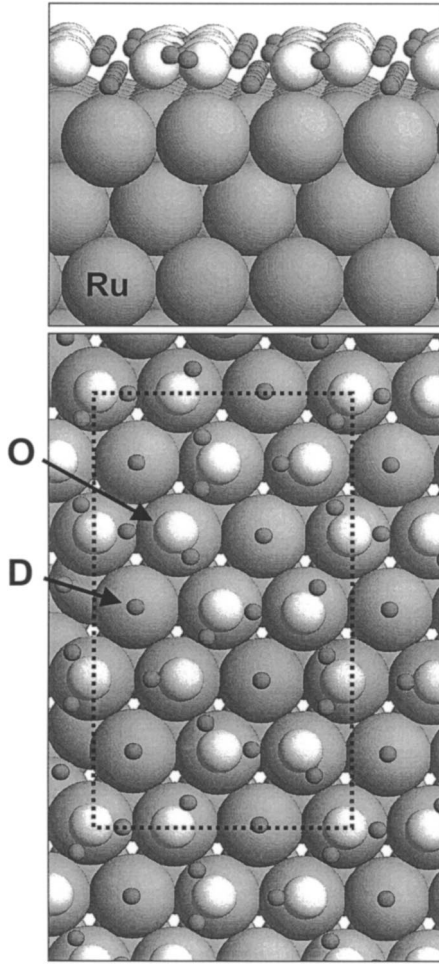


FIG. 2. A half-dissociated $D_2O/Ru(0001)$ adsorption geometry. Arrows identify the atom species. Lower panel: Top view, showing the non-H-bonding D atoms of the bilayer moved to atop-Ru-atom sites. The dotted rectangle indicates the $3 \times 3\sqrt{3}$ unit cell chosen to allow equal populations of OD-bond orientations. In a $\sqrt{3} \times \sqrt{3}-R30^\circ$ cell, all D_2O 's would have the same orientation, and so would all OD's. Upper panel: Side view, showing that the O atoms are close to coplanar.

This approximation underestimates O vibration frequencies because they scale as the inverse square root of the *reduced* O mass. However, O-Ru interaction not only increases the O vibration rate but also reduces Ru surface vibration frequencies—a “level repulsion” effect. A simple coupled-oscillator model described herein implies that this compensation of effects reduces the error in the sum of the vibration frequencies, introduced by fixing the Ru atoms, to $\sim 2\%$, for O-metal stretch modes. Based on the behavior of an isolated O-Ru diatomic molecule, one might have expected an 8% error.

The commutativity of partial derivatives, i.e., the identity $\partial^2 E / (\partial r_i \partial r_j) \equiv \partial^2 E / (\partial r_j \partial r_i)$, where the indices i and j refer to Cartesian coordinates, means the harmonic dynamical matrix is symmetric, i.e., $dF_x/dy = dF_y/dx$, $dF_y/dz = dF_z/dy$, and $dF_z/dx = dF_x/dz$. However, these symmetry conditions are not automatically satisfied in the VASP calculations, because forces are computed analytically, via the

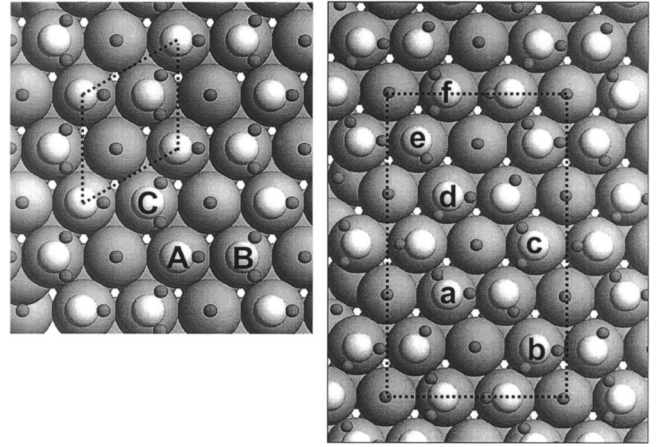


FIG. 3. Top views of half-dissociated D_2O adlayers on $Ru(0001)$ optimized with VASP. Left panel: A $\sqrt{3} \times \sqrt{3}-R30^\circ$ adlayer. Right panel: A $3 \times 3\sqrt{3}$ structure. In the former, the inter-O-atom distances are $\overline{AB} = 2.87$ and $\overline{AC} = 2.65$ Å. In the latter, $\overline{ab} = 4.77$, $\overline{ad} = 4.57$, $\overline{ed} = 2.92$, and $\overline{ef} = 2.62$ Å, while $\angle abc = 57.1^\circ$ and $\angle adc = 59.6^\circ$. Formally, to the extent that $\angle abc$ and $\angle adc$ do not equal 60° , or equivalently, that $\overline{ab} \neq \overline{ad}$, the diffraction pattern produced by the O atoms of the right panel structure will differ from $\sqrt{3} \times \sqrt{3}-R30^\circ$. See discussion in Sec. III.

Hellmann-Feynman theorem, but force derivatives are obtained by numerical differentiation. I therefore enforce dynamical-matrix symmetry “by hand,” before solving the Hooke’s law dynamical equations, by replacing each of the calculated values of dF_i/dr_j and dF_j/dr_i by their average.

Dynamic dipole moments of the various vibration modes govern the intensities of the associated loss features in infrared-absorption and specular electron energy-loss spectroscopies. These moments are characterized by an effective charge e^* , which I compute in terms of the changes in work function ϕ with the height z of each adatom in the unit cell. The effective charge associated with displacement of atom i is, specifically,

$$e_i^*/e = A/(4\pi H a_o) d\phi/dz_i, \quad (1)$$

where e is the electron charge, H is 1 hartree ($=27.2$ eV), a_o is the bohr radius, and A is the area of the surface unit cell.

To determine how the height of each atom in the unit cell changes for any particular vibration mode, I begin from the Hooke’s law eigenvalue equation

$$M_i \omega^2 \mathbf{r}_i = \sum_j D_{i,j} \mathbf{r}_j, \quad (2)$$

in which M_i and \mathbf{r}_i are the mass and position vector of the i th atom, ω is the angular vibration frequency, and $D_{i,j} \equiv -\partial \partial / (\partial r_j \partial r_i) E$ is the dynamical matrix. Defining

$$\mathbf{u}_i \equiv M_i^{1/2} \mathbf{r}_i, \quad (3)$$

Hooke’s equation assumes the symmetric form

$$\omega^2 \mathbf{u}_i = \sum_j D_{i,j} M_i^{-1/2} M_j^{-1/2} \mathbf{u}_j. \quad (4)$$

The solution to this eigenvalue problem is a set of eigenvectors and eigenvalues $\{\mathbf{u}_i^{(n)}, \omega_i^{(n)}\}$, from which I compute the effective charge of mode n as

$$e^{(n)*}/e = A/(4\pi H a_o) \sum_i M_i^{-1/2} \zeta_i^{(n)} d\phi/dz_i, \quad (5)$$

where $\zeta_i^{(n)}$ is the z component of the normalized eigenvector $\mathbf{u}_i^{(n)}$.

Finally, to compute vibration frequencies and estimate the zero-point energy of bulk ice-Ih in comparison to water adlayers, I performed VASP calculations for Hamann's "Bernal-Fowler ice model,"²¹ containing 12 water molecules in a hexagonal unit cell (six in each of two stacked bilayers). Describing O and D (or H) nuclei with ultrasoft pseudopotentials, and using a $3 \times 3 \times 2$ sample of the bulk Brillouin zone, the dimensions of the cell optimize to $7.62 \times 7.62 \times 7.17$ Å, with an O-O separation of 2.69 Å. Again I confined the phonon calculation to the Γ point, now of the *bulk* Brillouin zone.

III. WHAT CHOICE OF UNIT CELL BEST DESCRIBES $\text{D}_2\text{O}/\text{Ru}(0001)$?

Although Held and Menzel's pattern of LEED beams^{4,22} implies a $\sqrt{3} \times \sqrt{3}$ - $R30^\circ$ adlayer, if one takes this periodicity literally, the OD bonds on each D_2O must be oriented identically, and similarly for the OD fragments (see Fig. 3, left panel). More likely, the O-D bonds forming the half-dissociated adlayer are random, or "glassy," only producing the observed $\sqrt{3} \times \sqrt{3}$ - $R30^\circ$ LEED pattern on average.

Performing calculations for the larger, $3 \times 3\sqrt{3}$ cell (Fig. 3, right panel) gives some insight into the effects on the vibration spectrum of random orientation of the O-D bonds. In this cell, though the D_2O 's and OD's are obviously not random, but highly ordered, for each O-D bond pointing along a particular direction, there is another of the same type rotated by 120° (see Fig. 3, right panel). This arrangement is accordingly more consistent with reality, a notion supported by the VASP finding (see Table 3 of Ref. 5) that the D_2O adsorption enthalpy is 30 meV greater in the $3 \times 3\sqrt{3}$ structure.

As noted below, vibration features computed for the $3 \times 3\sqrt{3}$ cell are somewhat shifted relative to those of the $\sqrt{3} \times \sqrt{3}$ - $R30^\circ$ adlayer. The reason is that, as indicated in the caption to Fig. 3, O-O separations are somewhat different in the $3 \times 3\sqrt{3}$ cell. In a truly random arrangement of O-D bonds, there should be a spectrum of O-O separations, and therefore not just a shift, but also a broadening of vibration features.

It should be emphasized that the $3 \times 3\sqrt{3}$ cell represents nothing more than a *model* of the effects of random O-D-bond orientation. If this molecular arrangement actually existed on Ru(0001), Held and Menzel would have seen extra LEED spots, reflecting its O-O nearest-neighbor distances that are not all equal and its O-O-O angles that are not 60° and 120° . That no such extra spots were seen implies either the unlikely possibility that the O-D bonds of the adlayer were completely ordered, as in the left panel of Fig. 3, or the much more likely possibility that the O-D bonds were random, washing out any extra LEED beams.

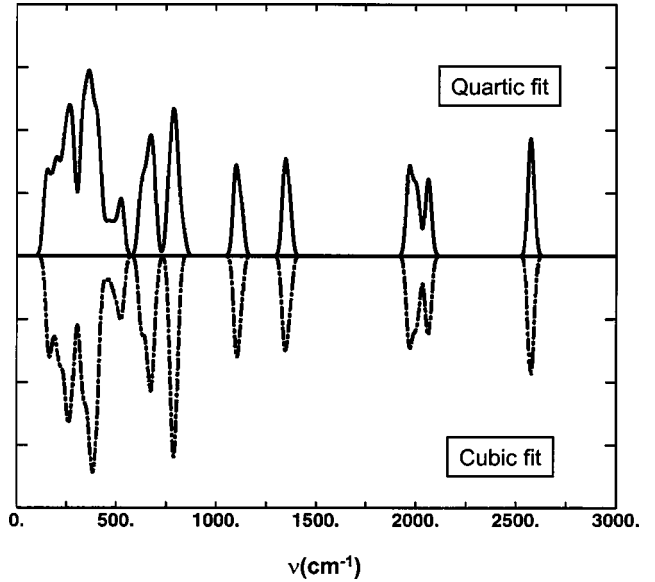


FIG. 4. Comparison of vibrational densities of states (smoothed by folding with a Gaussian of half width 20 cm^{-1}) for the half-dissociated $3 \times 3\sqrt{3}$ overlayer of Fig. 2, using quartic (solid line) vs cubic (dash-dotted line) fits to the force data. The latter has been flipped for clarity.

IV. COMPUTED VIBRATION SPECTRA

I begin the presentation of numerical results with tests of the accuracy of the various approximations described in Sec. II. Then, I discuss the GGA vibration spectra in comparison with experiment.

A. Tests of accuracy

A basic issue is the accuracy of a dynamical matrix obtained by polynomial fitting to force vs displacement results, and then symmetrizing by hand. Figure 4 compares vibration spectra obtained for the partially dissociated $3 \times 3\sqrt{3}$ overlayer of Fig. 2, using quartic vs cubic fits to the force data. That the results are very similar shows that noise in the fit data (which afflicts the evaluation of some of the smaller dynamical-matrix elements) is unimportant.

In Fig. 5, for a half-dissociated $\sqrt{3} \times \sqrt{3}$ - $R30^\circ$ overlayer, I compare vibration spectra computed with the USP description of electron-nucleus interactions, and with a more accurate PAW description using a high plane-wave cutoff. This figure shows clear differences between the less and more accurate calculations mainly among the low-frequency modes. Significantly, for the zero-point energy estimates discussed in the next section, the *mean* frequencies in the USP and PAW calculations differ by less than 1%.

To assess the error introduced by neglecting dispersion, i.e., by restricting vibration calculations to $\bar{\Gamma}$ in the SBZ, I compare the spectrum of a half-dissociated $\sqrt{3} \times \sqrt{3}$ - $R30^\circ$ D_2O overlayer, in Fig. 6, with the same computed after setting all intermolecular dynamical-matrix elements to zero. Not surprisingly, the figure shows that the high-lying intramolecular bend and stretch frequencies are essentially unaffected by these matrix elements. There are, however, no-

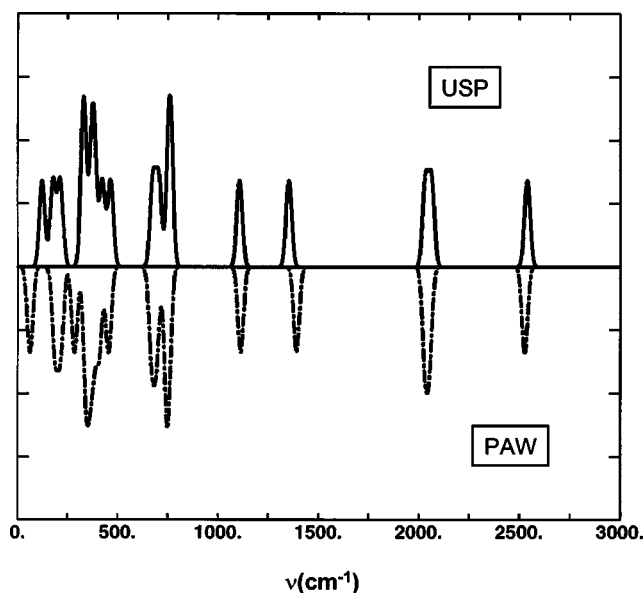


FIG. 5. The vibrational density of states of a half-dissociated $\sqrt{3} \times \sqrt{3}$ - $R30^\circ$ D₂O overlayer on Ru(0001), computed with the USP description of electron-nucleus interactions and a 29.1 Ry plane-wave cutoff (solid line), versus the same computed using the PAW method and a 51 Ry cutoff (dash-dotted line). In both cases the density of states has been smoothed by folding with a Gaussian of half width 20 cm⁻¹. The latter is flipped for clarity.

table effects of intermolecular coupling at 700 cm⁻¹ and below, implying that more extensive calculations are needed before comparing theory and experiment in this regime. Despite the shifts produced by intermolecular matrix elements, it should be noted that the mean vibration frequency changes by only $\sim 1\%$ when these elements are set to zero. This means that confining calculations to $\bar{\Gamma}$ will affect an estimate of zero-point energy only to this small extent.

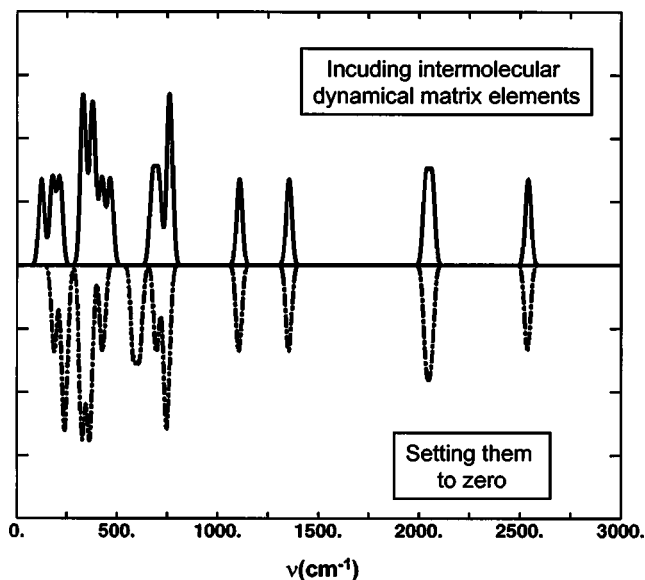


FIG. 6. The vibrational density of states of half-dissociated $\sqrt{3} \times \sqrt{3}$ - $R30^\circ$ D₂O/Ru(0001) (solid line) compared to the same computed after dropping all intermolecular dynamical-matrix elements (dash-dotted line). The latter has been flipped for clarity.

It is important to appreciate that weak dispersion in intramolecular vibration bands does not mean that the frequencies of these modes are insensitive to intermolecular separation. The potential in which an H-bonding D or H vibrates is flatter if the O atoms adjacent to it are closer together. This explains why the stretch modes of the OD fragments in a half-dissociated layer lie as high as 2586 cm⁻¹ in the results for the $3 \times 3\sqrt{3}$ unit cell, but only at 2540 cm⁻¹ with the $\sqrt{3} \times \sqrt{3}$ - $R30^\circ$ cell (see Table I). The difference is that in the larger unit cell, the O-O separation (\overline{ed} , in Fig. 3) for the donor bond from the OD fragment to the adjacent D₂O is 2.92 Å. In the smaller cell the same bond (\overline{AB} , in Fig. 3) corresponds to a 2.87 Å O-O separation. The shorter bond, as expected, produces a lower stretch frequency.

Beyond numerical accuracy issues, a last question concerns the basic physical approximation: To what degree does the GGA yield reliable vibration frequencies for condensed water systems? According to inelastic incoherent neutron-scattering results for polycrystalline (H₂O) ice-Ih,²³ intramolecular bending and two stretch bands are centered at 1613, 3203, and 3340 cm⁻¹. The GGA results for the mean bending and stretch frequencies, using Hamann's ice-Ih model²² and the USP description of electron-nucleus interactions, are 1643, 3020, and 3242 cm⁻¹. Thus, the computed vibration frequencies appear accurate to 2%–3% despite the systematic error inherent in the GGA exchange-correlation energy and the various numerical approximations described in the previous section.

B. Calculated vibrations of water on Ru(0001) vs experiment

A hint that molecular dissociation occurs among the first water molecules deposited on Ru(0001) already appeared in Thiel, DePaola, and Hoffmann's 1984 EELS results for H₂O/Ru(0001).⁷ In particular, the 3680 cm⁻¹ feature these authors observed on an ice multilayer annealed to 80 K was absent when only a single "bilayer" was left at 165 K.

SFG experiments on an ice-Ih crystal place the free OH stretch at 3695 cm⁻¹.²⁴ Similarly, and lending credibility to the GGA's accuracy, the GGA vibration spectrum for a bilayer of intact H₂O molecules (as in Fig. 1) includes a free OH stretch at 3720 cm⁻¹.²⁵ If, based on these results, one infers that Thiel, DePaola, and Hoffmann's 3680 cm⁻¹ mode is the multilayer's free OH stretch, then, following the logic of Denzler *et al.*,⁶ its absence when only the last water adlayer remains on the metal means that *this adlayer has no non-H-bonding H atoms*. All its H atoms are either bound to Ru's or participate in H bonding, as in a half-dissociated wetting layer.

Implicitly contradicting this reasoning, however, Thiel, DePaola, and Hoffmann interpreted the multilayer's 3680 cm⁻¹ feature not as the free OH stretch, but as a two-phonon excitation involving a 230 O-O and a 3420 cm⁻¹ O-H stretch.⁷ Since the 230 cm⁻¹ mode is also absent when only a "bilayer" is left on the surface, it can no longer participate in a combination band. Thus one can understand the disappearance of the 3680 cm⁻¹ mode without appealing to a half-dissociated wetting layer. On the other hand, one then

TABLE I. Calculated average frequencies versus O-O separation, of the essentially intramolecular O-D stretch bands of OD and D₂O in half-dissociated overlayers of D₂O/Ru(0001). In each case, the vibrating D atom(s) belong to the donor species. For the D₂O-associated bands, the labels “sy” and “as” denote the symmetric and asymmetric stretch modes [see, e.g., P. A. Thiel and T. E. Madey, *Surf. Sci. Rep.* **7**, 211 (1987), Fig. 1].

Unit cell	Donor species	Donor label, in Fig. 3	O-O separation (Å)	$\bar{\nu}$ (cm ⁻¹)
$\sqrt{3} \times \sqrt{3}$ -R30°	OD	A	2.87	2540
$\sqrt{3} \times \sqrt{3}$ -R30°	D ₂ O	C	2.65	2064 (as), 2034 (sy)
$3 \times 3\sqrt{3}$	OD	e	2.92	2576
$3 \times 3\sqrt{3}$	D ₂ O	f	2.62	2046 (as), 1976 (sy)

needs to explain why the free OH stretch is ~ 200 cm⁻¹ lower in the EELS spectrum of Ref. 7 than in the SFG data of Ref. 24.

Incidentally, Thiel, DePaola, and Hoffmann support the contention that the 3680 cm⁻¹ feature is a combination band by pointing to its relatively low intensity,⁷ in contrast to the large Born effective charge and high intensity expected of a free OH stretch.²⁶ However, the number of free OH bonds at Thiel, DePaola, and Hoffmann’s multilayer surface is not known, nor is their spatial orientation. Thus, interpreting the EELS peak intensity is not trivial.

Similar problems of interpretation arise for modes of the *first* adsorbed layer of H₂O/Ru(0001). In LEED, this system shows itself to have a complicated misfit dislocation structure.^{22,27,28} This means H₂O molecules are present on the surface in numerous bonding environments, making a persuasive comparison of theoretical and experimental vibration spectra difficult at best. For D₂O/Ru(0001), by contrast, what made Held and Menzel’s structure analysis feasible was that a careful anneal produced a sharp $\sqrt{3} \times \sqrt{3}$ -R30° pattern of LEED beams.^{4,22} Thus, apart from randomness of OD orientations, there are only two D₂O-bonding environments in Held and Menzel’s adsorption structure, and this is the system of choice for further study of the water/Ru(0001) vibration spectrum. Until now, however, a detailed EELS measurement has not been published for D₂O/Ru(0001). What is available is the SFG study of Denzler *et al.*, covering a rather narrow range of frequencies.⁶

Specifically, Denzler *et al.* measured SFG between 2560 and 2850 cm⁻¹ during a slow (0.05 K/s) thermal ramp, in which several layers of D₂O evaporated from a Ru(0001) sample. With the multilayer still present at 140 K, the only prominent feature in the SFG spectrum was a large peak centered at 2730 cm⁻¹, attributed to a free OD stretch.²⁹ As the temperature of the sample rose through the multilayer desorption feature, the intensity of this peak dropped, and at 157 K, where only the last layer of D₂O remained on the surface, the 2730 cm⁻¹ mode was no longer observable.⁶ Thus, Denzler *et al.* inferred that in the last layer of D₂O, there are no non-hydrogen-bonding D atoms.

The present calculations favor this reasoning. In Fig. 7, for example, I compare the spectra computed for the intact and half-dissociated $\sqrt{3} \times \sqrt{3}$ -R30° D₂O/Ru(0001) structures of Figs. 1 and 2. Note that for the intact-molecule structure, with a free OD in each unit cell, the highest-frequency vibration is the free OD stretch mode at 2706 cm⁻¹, i.e., within a few wave numbers of the measured free OD stretch. In the half-dissociated adsorption structure, the highest peak lies instead at 2540 cm⁻¹, below the range of Denzler *et al.*’s observations. It corresponds to the stretch vibration of an H-bonded OD fragment. In the bonding arrangement of the $3 \times 3\sqrt{3}$ unit cell (see Fig. 3) this mode is shifted up to 2586 cm⁻¹, because the O-O separation of the OD donor bond is longer than in the $\sqrt{3} \times \sqrt{3}$ -R30° cell. This is not high enough to account for the weak SFG feature Denzler *et al.* observed at 2650 cm⁻¹. Whether that is a discrepancy pointing to a systematic error of the GGA, or it indicates a too-

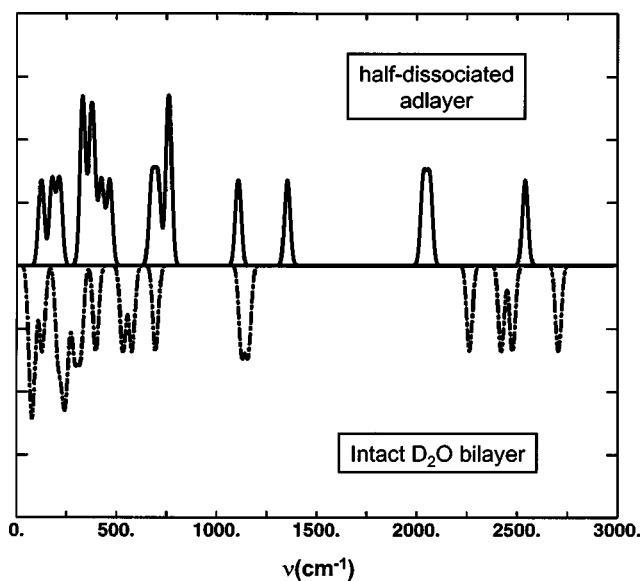


FIG. 7. Comparison of the spectra computed for the intact (solid line) and half-dissociated (dash-dotted line) $\sqrt{3} \times \sqrt{3}$ -R30° D₂O/Ru(0001) structures of Figs. 1 and 2. In both cases the density of states has been smoothed by folding with a Gaussian of half width 20 cm⁻¹. The latter has been flipped for clarity.

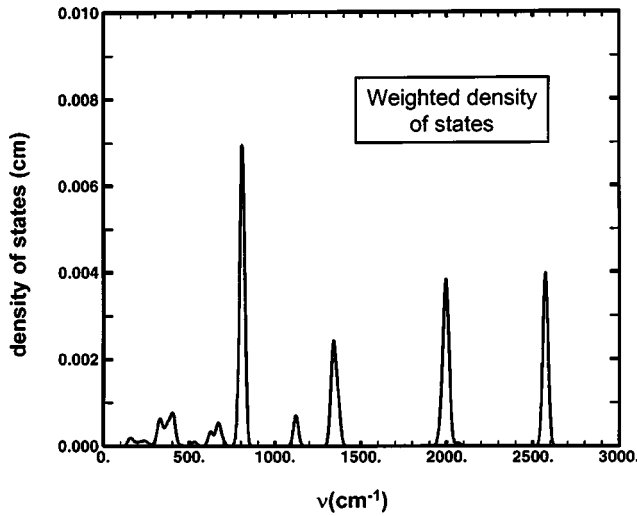


FIG. 8. Density of states weighted by $[e^{(n)}/e]^2$ for the half-dissociated $3 \times 3\sqrt{3}$ D₂O adlayers of Fig. 3. The state densities have been smoothed by folding with a Gaussian of half width 20 cm^{-1} .

unrealistic model distribution of OD-bond orientations is not yet clear.

To this point, the figures representing vibration spectra (Figs. 4–7) have been density-of-states plots. In Fig. 8, I have weighted the densities of states of the half-dissociated $3 \times 3\sqrt{3}$ D₂O adlayers by $[e^{(n)}/e]^2$, calculated according to Eq. (5), with parabolic fits to VASP work functions to obtain $d\phi/dz$. Figure 8 makes it plain that there are dipole-active OD stretch modes for a half-dissociated layer, even though their OD bonds all lie parallel to the surface. These modes belong to the totally symmetric representation of the rotation group of the Ru(0001) surface, and should be visible in infrared-absorption and specular electron energy-loss spectroscopies.³⁰

V. ZERO-POINT ENERGIES

Calculations of vibration spectra not only help identify the water adsorption structure on Ru through comparison with measurements. They also make it possible to correct computed classical heats of adsorption for quantum contributions attributable to zero-point motion, which is the focus of what follows.

A. Theoretical issues

Replacing a stiff O-D (or O-H) bond with a softer metal-D (or metal-H) bond reduces the value of $1/2 \sum \hbar \omega$. This is good reason to surmise that, overall, zero-point energy stabilizes a half-dissociated adlayer relative to structures made uniquely of intact water molecules. However, other effects might intervene. One is that dissociation of a water molecule might stiffen or give rise to other modes, compensating or even overcompensating for the replacement of the O-D stretch with a softer mode, in the summation. An obvious candidate in the present case is the O vibration mode shifted to higher frequency because the OD fragment produced by the dissociation forms a new O-metal bond.

An overcompensation of this nature explains why zero-point energy *opposes* formation of ice from water molecules even though the O-H stretch is softer for water molecules in the solid than in the vapor phase. The countervailing effect in ice is that the isolated water molecule can rotate freely, whereas its rotation in the solid is hindered. Because the sum of the hindered rotation frequencies exceeds the softening of the stretch modes, ice binding is reduced rather than enhanced by quantum effects. Whether an effect like this occurs in the case of adsorption layers is tested here by calculating and comparing frequency sums.

Another concern in estimating zero-point effects is the importance of substrate atom motion. It requires much less effort to compute the vibration modes of a layer of ice on a rigid Ru(0001) slab than on one whose Ru atoms can move. However, the O/Ru mass ratio $16/101=0.158$ is not infinitesimal. So, the easier calculation is suspect without an error estimate.

For an O-Ru dimer in the gas phase, the error is governed by the reduced mass, $m_{\text{O}m_{\text{Ru}}}/(m_{\text{O}}+m_{\text{Ru}})=13.81$ compared to $m_{\text{O}}=16$, shifting the dimer stretch upwards by 7.6%. However, for water adsorption on a Ru crystal, the shift of an O-Ru stretch mode will be in the opposite direction to the shift of the Ru phonon to which it couples, a typical level-repulsion effect. One may therefore expect a smaller error than 7.6% in the zero-point energy sum for water vibrating on a Ru crystal.

The largest effects of finite m_{Ru} should involve coupling of O-Ru stretch modes to Ru surface vibrations near the Ru phonon band edge, where neighboring Ru atoms oscillate against each other. One reason is that the computed O-Ru stretch mode frequencies lie near $400 \text{ cm}^{-1}=50 \text{ meV}$, close to the upper limit of the Ru vibration band, i.e., the Debye temperature of $600 \text{ K}=52 \text{ meV}$. Another is that acoustic vibrations of the metal correspond to many Ru atoms moving essentially as a block, making the effective mass of the object against which the O vibrates considerably larger than the mass of a single Ru atom.

Consider, therefore, a simple model of an O atom in near resonance with a band-edge phonon, namely, an O-Ru dimer tethered to an infinitely massive “rest of the Ru crystal,” to estimate the finite-Ru-mass error. Assigning the natural frequencies ω_A and ω_S (where “A” stands for adsorbate and “S” for substrate) to the O-Ru and Ru “rest-of-the-crystal” springs, and defining $x \equiv \omega_S/\omega_A$ and $r \equiv m_{\text{O}}/m_{\text{Ru}}=0.158$, the vibrations of the coupled system occur at frequencies

$$\omega_{\pm} = (\omega_A^2(1+r)/2 + \omega_S^2/2 \pm \{[\omega_A^2(1+r) + \omega_S^2]^2/4 - \omega_A^2\omega_S^2\}^{1/2})^{1/2}, \quad (6)$$

and the relative shift in the sum of the O-Ru and Ru “rest-of-the-Ru-crystal” frequencies is

$$R(x,r) = (\{(1+r+x^2)/2 + [(1+r+x^2)^2/4 - x^2]^{1/2}\}^{1/2} - \{(1+r+x^2)/2 - [(1+r+x^2)^2/4 - x^2]^{1/2}\}^{1/2})/(1+x). \quad (7)$$

TABLE II. Zero-point energy estimated for ice-Ih and for various periodic water overlayers on Ru(0001), and the corresponding wetting preference enthalpies. The classical energies (or “lattice energies”) are from Ref. 5. The wetting preference enthalpies, in the last column, are obtained by summing the previous two columns and subtracting the ice-Ih result.

System	Unit cell	Constituent	Classical energy (eV)	Zero-point energy (meV)	Total vs ice-Ih (eV)
Ice-Ih	$3 \times 3 \times 2^a$	D ₂ O	-0.72	96	0
Bilayer	$\sqrt{3} \times \sqrt{3} - R30^\circ$	D ₂ O	-0.52	75	+0.18
1/2 dissociated layer	$\sqrt{3} \times \sqrt{3} - R30^\circ$	D ₂ O	-0.71	40	-0.05
1/2 dissociated layer	$3 \times 3\sqrt{3}$	D ₂ O	-0.74	41	-0.08
Ice-Ih	$3 \times 3 \times 2^a$	H ₂ O	-0.72	124	0
Bilayer	$\sqrt{3} \times \sqrt{3} - R30^\circ$	H ₂ O	-0.52	94	+0.17
1/2 dissociated layer	$\sqrt{3} \times \sqrt{3} - R30^\circ$	H ₂ O	-0.71	41	-0.07
1/2 dissociated layer	$3 \times 3\sqrt{3}$	H ₂ O	-0.74	43	-0.10

^aHere the “ 3×3 ” is intended to parallel the unit-cell definitions used for the water overlayers on Ru(0001). This ice-Ih cell contains two hexagonally stacked bilayers each containing six water molecules.

At resonance, $x = 1$, and $R(1,0.158) \approx 1.02$. This means that setting the Ru mass to ∞ underestimates the O-Ru stretch contribution to the zero-point energy sum by about 2%, or about 0.5 meV per 50 meV stretch mode.³¹

The remaining question concerning the accuracy of the computed zero-point energy sum involves anharmonicity. The zero-point energy contributed by a vibration whose ground-state amplitude swings outside the range where the restoring force is given by Hooke’s law should be computed by solving an anharmonic equation of motion. Typically, this would be expected to occur for soft modes whose zero-point contributions are small whether or not anharmonicity is accurately taken into account.

B. Numerical results for zero-point energies of various water structures

In Table II, zero-point energy contributions to cohesion are given for several structures. For each arrangement of water molecules, the energy quoted was obtained by subtracting the experimental zero-point energy of the D₂O molecule, 419 meV,³² from the GGA value of $1/2 \sum \hbar \omega$, calculated without a finite-Ru-mass correction.

As anticipated, the half-dissociated adlayer on Ru(0001) has a lower zero-point energy than the bilayer of intact water molecules, stabilizing the dissociated arrangement. The difference, 35 meV for heavy water, is substantial compared to the low temperatures $< 159 \text{ K} = 13.7 \text{ meV}$, at which the $\sqrt{3} \times \sqrt{3} - R30^\circ$ layer is observed.

Nonetheless, the zero-point energy difference is not uniquely a consequence of eliminating an O-D stretch mode from the sum and replacing it with a Ru-D stretch. This would favor the half-dissociated adlayer by 42 meV.

As noted above, the O-Ru stretch modes in the half-dissociated layer have frequencies in the neighborhood of 50 meV. The dissociation of one D₂O per cell to form adsorbed

OD and D fragments thus adds about 13 meV per molecule to the zero-point energy burden of the half-dissociated structure. This would increase by $\sim 0.5 \text{ meV}$ if the finite Ru mass had been taken into account, according to the estimate in the previous paragraphs.

Table II also shows the result of a zero-point energy calculation for ice-Ih, 96 meV/D₂O. This value, which is satisfyingly close to Whalley’s estimate of 98 meV based on measured vibration spectra,³³ implies that zero-point contributions favor the formation of wetting layers, whether of intact or dissociated molecules. In particular, the half-dissociated structure gains 57 meV relative to three-dimensional ice-Ih—or perhaps slightly less, as discussed, due to the finite-Ru-mass effect. This means that quantum effects break the near equality of the half-dissociated layer’s heat of adsorption on Ru(0001) and the sublimation of ice, and significantly promote the observed wetting.

VI. RECAPITULATION

Agreement at the level of $\sim 1\%$ between calculated and observed “free” OD and OH stretch vibration modes for water on Ru(0001) underlines the reliability of GGA total energies as a tool for diagnosing the adsorbed water layer structure. Thus, obtaining and comparing EELS data for $\sqrt{3} \times \sqrt{3} - R30^\circ$ D₂O/Ru(0001) to the theoretical spectra presented here would provide a meaningful test of the reality of a half-dissociated wetting layer as the explanation for Held and Menzel’s surprisingly compressed “bilayer.” Estimates show that zero-point energy stabilizes the half-dissociated layer, largely because a stiff OD bond is replaced by a soft Ru-D bond when dissociation occurs. Zero-point stabilization of a bilayer of *intact* D₂O molecules is too weak to allow it to wet Ru(0001).

ACKNOWLEDGMENTS

I am grateful to D. N. Denzler for alerting me to his SFG results prior to publication, and to D. L. Mills and N. C. Bartelt for helpful conversations. This work was supported in

part by the Department of Energy (DOE) Office of Basic Energy Sciences, Division of Material Sciences. Sandia is a multiprogram laboratory operated by Sandia Corporation, a Lockheed-Martin Company, for the U.S. DOE under Contract No. DE-AC04-94AL85000.

- ¹P. Hohenberg and W. Kohn, Phys. Rev. **136**, 864 (1964); W. Kohn and L. J. Sham, Phys. Rev. A **140**, 1133 (1965).
- ²J. P. Perdew, in *Electronic Structure of Solids '91*, edited by P. Ziesche and H. Eschrig (Akademie Verlag, Berlin, 1991); J. P. Perdew, J. A. Chevary, S. H. Vosko, K. A. Jackson, M. R. Pederson, D. J. Singh, and C. Fiolhais, Phys. Rev. B **46**, 6671 (1992).
- ³M. A. Henderson, Surf. Sci. Rep. **46**, 1 (2002).
- ⁴G. Held and D. Menzel, Surf. Sci. **316**, 92 (1994).
- ⁵P. J. Feibelman, Science **295**, 99 (2002).
- ⁶D. N. Denzler, Ch. Hess, R. Dudek, S. Wagner, Ch. Frischkorn, M. Wolf, and G. Ertl, (unpublished).
- ⁷P. A. Thiel, R. A. DePaola, and F. M. Hoffmann, J. Chem. Phys. **80**, 5326 (1984).
- ⁸G. Kresse and J. Hafner, Phys. Rev. B **47**, 558 (1993).
- ⁹G. Kresse and J. Hafner, Phys. Rev. B **49**, 14 251 (1994).
- ¹⁰G. Kresse and J. Furthmüller, Comput. Mater. Sci. **6**, 15 (1996).
- ¹¹G. Kresse and J. Furthmüller, Phys. Rev. B **54**, 11 169 (1996).
- ¹²D. Vanderbilt, Phys. Rev. B **41**, 7892 (1990).
- ¹³A. Pasquarello *et al.*, Phys. Rev. Lett. **69**, 1982 (1992).
- ¹⁴K. Laasonen *et al.*, Phys. Rev. B **47**, 10 142 (1993).
- ¹⁵G. Kresse and J. Hafner, J. Phys.: Condens. Matter **6**, 8245 (1994).
- ¹⁶G. Kresse and D. Joubert, Phys. Rev. B **59**, 1758 (1999).
- ¹⁷P. E. Blöchl, Phys. Rev. B **50**, 17 953 (1994).
- ¹⁸M. Methfessel and A. T. Paxton, Phys. Rev. B **40**, 3616 (1989).
- ¹⁹G. Kresse, computer code VASP guide (University of Vienna, Vienna, Austria, 1999), <http://cms.mpi.univie.ac.at/vasp/guide/node143.html>
- ²⁰J. Neugebauer and M. Scheffler, Phys. Rev. B **46**, 16 067 (1992).
- ²¹D. R. Hamann, Phys. Rev. B **55**, R10 157 (1997).
- ²²G. Held and D. Menzel, Phys. Rev. Lett. **74**, 4221 (1995).
- ²³J. Li, J. Chem. Phys. **105**, 6733 (1996), see Fig. 6.
- ²⁴W. Wei, P. B. Miranda, and Y. R. Shen, Phys. Rev. Lett. **86**, 1556 (2001); Q. Du, R. Superfine, E. Freysz, and Y. R. Shen, *ibid.* **70**, 2313 (1993).
- ²⁵The value is so high because the H atom in this bond does not lie between two O atoms, or, in other words, because there is no softening of the potential in which it oscillates associated with a second neighbor O (cf. Table I).
- ²⁶The effective charge computed from calculated changes in the work function as explained in Sec. II is $0.3e$. That suggests an EELS intensity per free OH bond is approximately 30 times larger than that of H on a metal surface. See, e.g., P. J. Feibelman and D. R. Hamann, Surf. Sci. **182**, 411 (1987) for a calculation of the latter.
- ²⁷G. Held and D. Menzel, Surf. Sci. **327**, 301 (1995).
- ²⁸E. D. Williams and D. L. Doering, J. Vac. Sci. Technol. A **1**, 1188 (1983).
- ²⁹The ratio of free OH and free OD stretch frequencies should roughly equal 1.37, including a correction for reduced mass. So if the free OH stretch is at 3695 cm^{-1} , one expects the free OD stretch to be at 2700 cm^{-1} .
- ³⁰See Y. R. Shen, Adv. Chem. Phys. **40**, 327 (1989) for a discussion of SFG selection rules.
- ³¹One must take into account that the zero-point energy sum has a factor of 1/2 in front of it.
- ³²B. T. Darling and D. M. Dennison, Phys. Rev. **57**, 128 (1940). Their value for H_2O is 574 meV.
- ³³E. Whalley, in *The Hydrogen Bond*, edited by P. Schuster, G. Zundel, and C. Sandorphy (North-Holland, Amsterdam, 1976), Vol. III, Chap. 29.